Coupled Electric Oscillators

Trevor Smith, Alex Storrer*
Northeastern University
(Dated: June 28, 2021)

In this lab, the behavior of single, uncoupled, and coupled LRC circuits were evaluated with simple relationships between L, R, C, and voltage as well as complex differential equations. The latter were simplified based on the unique initial conditions of this experiment. This behavior was further linked to a mechanical analogue, an elastic pendulum system. For two inductors, nearly identical behavior of the single RLC circuit was observed. The oscillating decay of the single LRC circuits were similar for the two inductors, where A-inductor and B-inductor were calculated to have decay natural frequencies of 14587.05± 0.03 rad/sec and 14578.44± 0.03 rad/s, and decay constants of 649.9± 0.1 s1 and 651.3± 0.1 s1. From these values the inductances were calculated to be 0.100±0.003 H for both of the inductors. When the A and B circuits were coupled via a coupling capacitor, each circuit produced a signal with a beat frequency of 170 ± 1 Hz. By using equations modeling a coupled LRC circuit, the coupling capacitance was calculated to be 4.1 ± 0.1 nF, which is one standard deviation away from its measured value of 3.9 ± 0.1 nF.

INTRODUCTION

In many circuits, a voltage is continuously applied to several components in series and/or in parallel. Three essential components used in circuits are resistors, capacitors, and inductors. These components operate in distinct ways, which can be seen by the way we use inductance, resistance, and capacitance to calculate voltage.

$$V = L \cdot \frac{d^2q}{dt^2}$$

$$V = R \cdot \frac{dq}{dt}$$

$$V = \frac{1}{C} \cdot q$$

Where V is voltage, L is inductance, R is resistance, C is capacitance, and q is charge. In other words, capacitors do work proportional to amount of charge buildup, resistors do work proportional to the flow of charge or current, and inductors do work proporional to the inflection of charge, or the change in current.

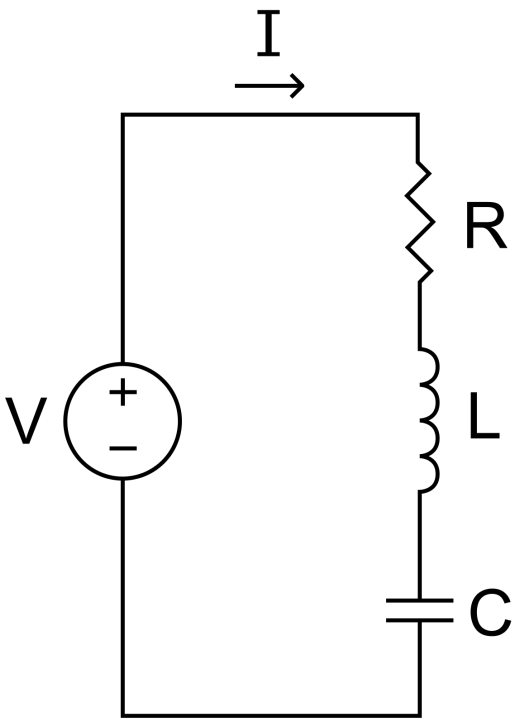

FIG. 1.

An LRC circuit, seen in 1, combines these three components to produce an oscillating response to any change in voltage, for example the turning on and off of an applied voltage. These oscillations could be compared to the oscillation of a spring-mass system, and indeed the differential equations describing both the voltage of an LRC circuit and the height of an oscillating spring/mass system in gravity look identical.

This peculiar behavior can be multiplied when two such systems interact with each other, behaving as what's known as "coupled oscillators". The beauty of differential equations is that a mathematical model can be used to describe such motion, even if the differential equation itself is unsolvable unless there are specific initial parameters. In an unsolvable case, a computer program can simulate the system one step at a time using Euler's method, or we can simply perform an experiment and let nature describe the motion. In this lab, we will be looking at a coupled electric oscillator that is operating in a normal mode, which is to say a mode where the coupled oscillators behave like a single harmonic oscillator, or a

solvable case.

APPARATUS

The apparatus consisted of the following.

- Coupled electronic oscillator circuit box
- Fixed capacitor, variable capacitor
- Two large inductor coils, labelled 'A' and 'B'
- Oscilloscope, Tektronix TDS210
- Digital Multimeter, Extech EX430A
- OpenChoice Desktop, Oscilloscope Software
- Jupyter, Python compiler
- LaTeX, document preparation software

MEASURE INDUCTANCE

Procedure

In this phase of the lab we measure the basic parameters of our system, described in 2, including L_A, L_B, R_{LA}, R_{LB}, full decay natural frequency ω_0, damping constant γ, time constant τ, quality factor Q and the standard capacitor. These values, save for the capacitance, are calculated by analyzing the voltage oscillations of the circuit. Values for R_{LA} and R_{LB} are also measured with an ohmmeter, and the capacitance is measured with a digital multimeter (DMM).

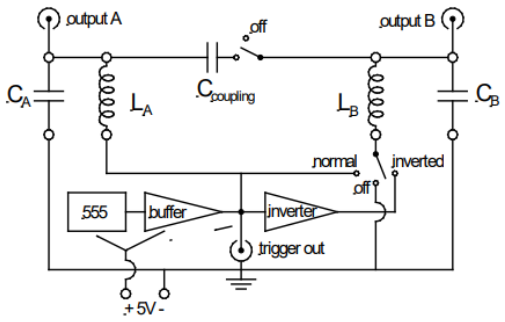

FIG. 2. Test setup for the coupled electric oscillators.

The standard capacitor and one inductor was installed in the A-circuit. A +5 VDC source was connected to the box, and the A-output was connected to channel 1 of an oscilloscope. The trigger out was connected to the scope trigger, and the viewing window of the scope was adjusted so that the decaying oscillation occurring when the square wave turns off was visible.

The decaying waveform is then stored digitally and analyzed. By using eq. 1 to make curve fits, the basic parameters of the system can be obtained. These fits were first performed on a single period of oscillation, in order to get an estimate without the added complexity of the exponential. Then, using the parameters for the sine wave as a starting point, the full equation describing the oscillation was obtained.

$$q(t) = q_0 e^{-\gamma t/2} cos(\omega_0 t) \tag{1}$$

Where q is charge as a function of time, γ is the decay constant, ω_0 is the natural frequency, and t is time. This equation, analogous to a mass-spring system being stretched and released, describes the flow of charge between the capacitor and inductor in the LRC circuit. When the 'spring is released', or the 555 pulse square wave switches off, the capacitor immediately discharges. However, the inductor counters such a quick change in current, and produces a current in the opposite direction, cancelling out a portion of the flow of charge from the capacitor. This has the effect of recharging the capacitor again, which, when the flow of current from the inductor is stopped, will again quickly discharge. The length of wire between the two circuit components, in this case, acts as a resistor and steadily gives off energy in the form of heat as a proportion of the current at a given moment. The end result is this beautiful equation describing a sine wave undergoing exponential decay.

This analysis was repeated with inductor 'B', inserted into the same circuit and replacing inductor 'A'.

Results

First, the capacitance of the standard capacitor was measured. The DMM has an uncertainty of 3% associated with all measurements, and yielded a capacitance measurement of 47 $\pm$ 1 μF.

A single period of the oscillation was recorded and analyzed for each inductor, shown in 3.

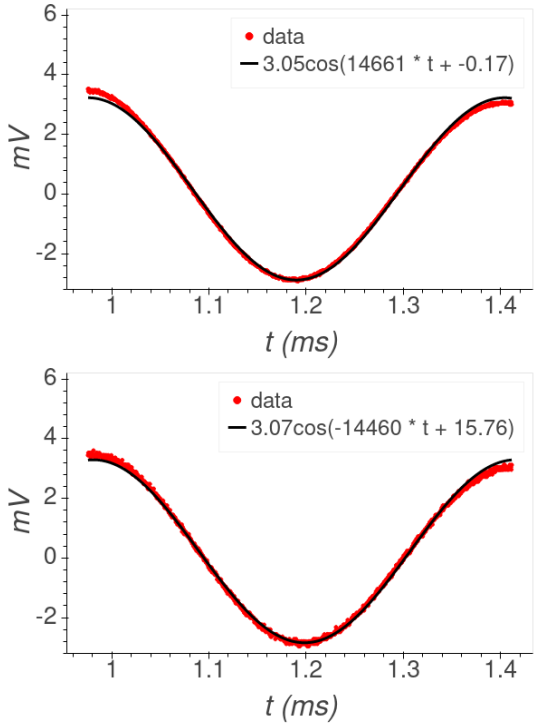

FIG. 3. Single period of oscillation and fit for A (above) and B (below). The differing fit parameters for phase and the sign of the frequency is not relevant in this case.

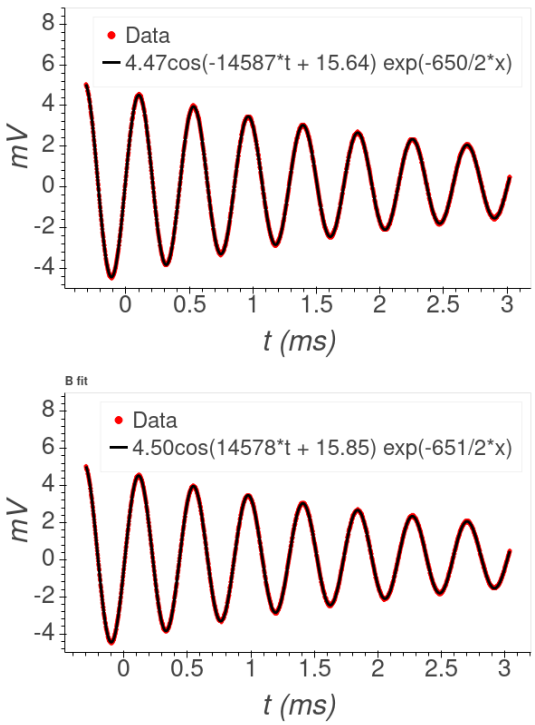

FIG. 4. Several periods of oscillations, with fit corresponding to eq. 1.

The calculated frequencies for A and B, respectively, are 14660 ± 30 Hz and 14460 ± 30 Hz, where the uncertainty is calculated from the covariance matrix of the fit. Using 2 and the values above, L_A and L_B were calculated to be 0.099 ± 0.003 H and 0.101 ± 0.003 H. It should be noted that the uncertainty in the fit was well below one part in 100, meaning that nearly all the uncertainty in the inductance measurements were due to the DMM.

$$L = \frac{1}{C\omega_0^2} \tag{2}$$

These fit parameters were then used as starting parameters for the more complicated curve fit needed when exponential decay is included, as shown in 4.

While the frequencies for A and B when viewing a longer decay were extremely precise, 14587.05 ± 0.03 and 14578.44 ± 0.03 respectively, the proportion of uncertainty in our calculated L values were exactly the same, caused again by uncertainty in the measured capacitance. These values did, however, agree better than before, at 0.100 ± 0.003 H for both inductors.

The damping coefficient γ was calculated at 650 /s and 651 /s for A and B respectively. This damping coefficient γ is related to the resistance R, which generates heat proportional to the flow of charge, and inductance L which generates a flow of charge opposite to the change in current, by eq. 3. We can then rearrange the equation so that we can use our calculated inductance and frequency to calculate resistance.

$$\gamma = \frac{R}{L} \rightarrow R = L\gamma \tag{3}$$

The resistance for inductor 'A' and 'B' were both found to be 65 ± 2 Ω. Again, calculations were precise enough to be able to distinguish a difference in the damping coefficient itself for the two inductors, but the error propagated from the DMM swamps that difference. This difference is small when considering the discrepancy between these calculated values for resistance and those measured directly with an ohmmeter. These measured resistances for inductor 'A' and 'B' were 17.4 ± 0.2 Ω and 17.2 ± 0.2 Ω respectively, with the error again coming from the DMM's 3% precision.

This difference can be attributed to a difference in exactly what is being measured. In the case of the DMM, the inductors were isolated from the circuit and measured separately, whereas the decay constant is caused by all resistance that exists in the circuit, including the wire and all contacts. Therefore, it is not surprising that the resistance related to the time constant is much higher.

In theory, this resistance does not have any effect on the frequency of the circuit, as ω_0 is clearly a function of only L and C.

Finally, two more important values were derived from values already discussed, τ, another to describe damping, called the time constant, and Q, or the quality factor, which also describes the decay in an oscillating system. The equations used for these values are given by 4 and 5 respectively. All constants in these equations have already been defined in this report.

$$\tau = \frac{2}{\gamma} \tag{4}$$

$$Q = \frac{\omega_0}{\gamma} \tag{5}$$

The quality factor for circuits containing each inductor 'A' and 'B' were again found to be equal after considering uncertainty due to the DMM, at 22.4 ± 0.7. This value corresponds to the amount of decay that occurs over a single period.

The time constant for circuits containing each inductor 'A' and 'B' calculated with great precision, as they do not depend on any measurements from the DMM. These values were 0.0030773 ± 0.0000006 s and 0.0030709 ± 0.0000006 s respectively. These uncertainties are $6.0 \cdot 10^{-7}$.

UNCOUPLED LRC OSCILLATORS

In the following sections, a system with two LRC circuits will be analyzed, starting with two uncoupled LRC oscillators. The B inductor and adjustable capacitor were then added to the B-circuit, and the B-circuit output was connected to channel 2 on the scope. By switching the coupling capacitor ***off***, these two LRC circuits were able to operate independently, but excited by the same emf pulse.

The waveforms were viewed on the oscilloscope, and the B-capacitor was adjusted until both waveforms had the same period. These waveforms were stored and are shown in fig. 5.

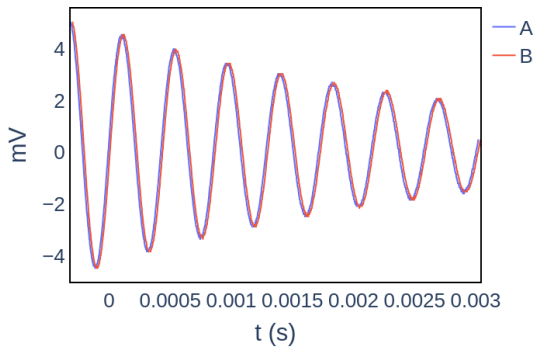

FIG. 5. Two uncoupled LRC circuits powered by the same pulse generator.

The variable capacitor was then removed from the circuit and measured with the DMM at 47 ± 1 nF. Considering that this value is exactly the same as the standard capacitor, and that the two inductances were the same within uncertainty, this makes sense. We would expect that, if all other parameters describing the oscillation are more or less equal, then in order to equalize the resulting waves then this parameter would need to be equal as well.

COUPLED LRC OSCILLATOR

In the final phase of this experiment, two coupled LRC oscillators are analyzed. The complexity of this system is drastically higher than a single oscillator, and as such the circuit has been designed in such a way to simplify the interaction of the two LRC circuits in terms of their phase. In the "normal" configuration, the amplitude of on oscillators are either the same or exactly opposite, corresponding to a phase difference of 0 or 180 degrees. In this configuration, the A-circuit begins at a maximum and the B-circuit begins at zero, corresponding to a 90 degrees phase difference. This is achieved by switching

"on" the coupling in our box, but switching "off" the trigger connection to the B-circuit.

Observing the "Beat"

Procedure

In this portion of the lab, we will observe the resulting output of the coupled LRC circuits and attempt to explain its behavior.

The variable capacitor was replaced in the B-circuit, and the box was set to the above stated parameters. As in the first section, the window of the scope was moved to observe only the falling edge of the excitation and the ensuing behavior of the two coupled circuits. The variable capacitor was tuned to reduce the minima between the resulting waves closest to zero as possible.

Results

The resulting waves were saved and analyzed digitally, and can be seen in 6.

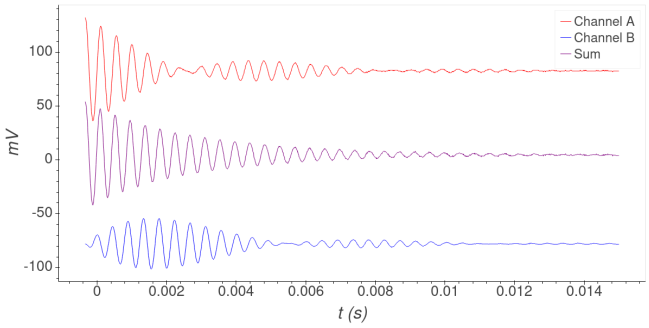

FIG. 6. Two coupled LRC circuits, operating at a 90 degree phase difference, and their sum.

We can see that the sum of the two channels produces a behavior very similar to the uncoupled or individual LRC circuits, but each coupled circuit, when measured individually, expresses a "beat" pattern.

Discussion

It is worth it to attempt to explain the behavior of the circuit before moving on. It seems clear that each time the A-capacitor discharges, most of the energy goes into the A-inductor and bounces back in the typical oscillating fashion seen above, but some of that energy goes into the B-circuit, producing a pattern of oscillation there. With each oscillation, more energy is moved into the B-circuit, but not as much energy is taken out of the B-circuit by its own oscillations, so the energy in the B-circuit steadily grows. At a certain point, the energy leaving the A-circuit is less than the energy leaving the B-circuit, and the pattern reverses, with the B-circuit losing energy to the A-circuit until the A-circuit reaches another maxima.

However, because the energy lost by a given circuit is more or less the same as the energy gained by the other one, the overall pattern of the sum of energy in the circuit is the same as a single oscillator. Therefore it is simply a translation of energy between two locations that produces this "beat".

Mechanical Analog

This behavior is still a little inscrutable, and therefore it is helpful to observe a mechanical analog which is more intuitively understood. This analog is a spring-mass system that is allowed to move in two dimensions, both up and down as well as side-to-side. A diagram describing this setup can be found in fig. 7.

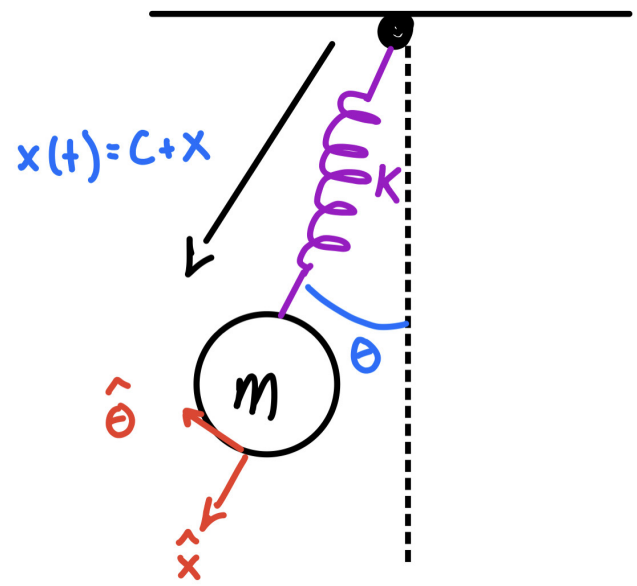

FIG. 7. Diagram of elastic pendulum coupled mechanical oscillator.

This system was setup in the lab, and a demonstration was made. The motion was initiated by simply adding tension to the string in the downward direction and releasing. What was observed was a component of the motion, very small at first, that was an angular,

pendulum motion rather than a spring motion, which grew slowly. At one point, this pendulum motion was the only motion observed, and the system by all means appeared to be a pendulum, for about one period. However, at the end of this period, some small spring motion was seen, which grew until the spring motion was the only motion observed and there was no angular momentum, as in the initial condition. This behavior then repeated several times.

This behavior is exactly like what was observed in the coupled LRC circuits, but the distinction between the two forms of energy was more profound. Instead of two waves that look similar, which are both described by the same equations and the same parameters, the mechanical demonstration clearly distinguished the exchange between the two forms of motion, angular and spring. We can more clearly understand why energy is exchanged between these two forms by thinking through it one step at a time, and we can draw parallels to the coupled LRC system.

First, the spring is drawn back and released, close to directly below the spring's mounting point. However, the mass is bound to be slightly off center in some direction. There is very little pendulum motion in that direction, but the accelerating spring gives a hard yank towards the mounting point. This yank is harder than regular string tension would be, if this was a regular pendulum, and the mass is kicked further out on the other side of the mounting point. The same thing happens for some time, until the spring is no longer providing a 'yank' to the mass because it is moving entirely in the pendulum mode with no motion toward or away from the spring mounting point. However, this simple harmonic motion can't be maintained because a spring does not provide the true tension force that is needed to produce continuous motion, and will stretch rather than provide a rigid restoring force. This stretching removes energy from the pendulum system, which will no longer sweep as far out. That pattern continues until the energy from the pendulum has been brought to zero, and we observe a spring motion only.

Fitting the "Beat"

In this section, numerical analysis is conducted on the digitized waveforms in order to calculate the coupling capacitance. First, analysis is simplified by fitting the inverse exponential to the sum of the two waves, and then dividing each wave by the exponential to remove the effect of the decay. This can be see in fig. 8.

By using two approaches to curve fitting the beats, the beat frequency and uncertainty were calculated. The

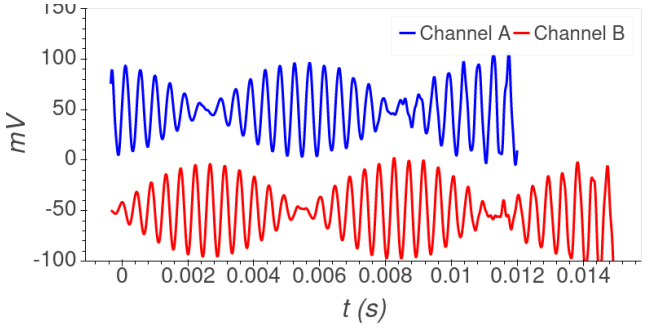

FIG. 8. The resulting A and B channel waves after removing the effect of the decay. A cutoff was chosen subjectively based on where the noise was greater than the signal.

first method involved taking the absolute value of the signal, and then extracting every peak. A simpler Hilbert transform approach was considered but the packet was not well defined enough for this purpose. These peaks were then fit to a cosine wave, providing a beat frequency for each wave.

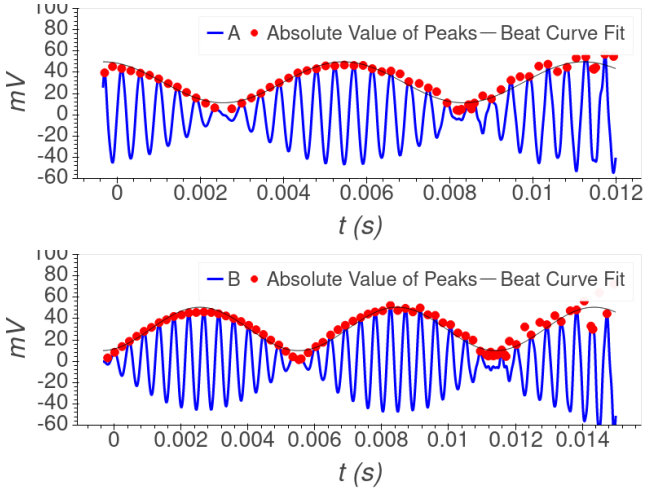

FIG. 9. Illustration of the peak fitting method of curve fitting the beats for both A and B channel waves, with Channel A shown above, and Channel B shown below.

The beat frequency for channel A was calculated at 168.34 Hz, and the beat frequency for channel B was calculated at 171.77 Hz.

The second method for finding this beat frequency utilizes Fourier analysis. The beat frequency is simply the difference between two dominant frequencies at work in the signal, and these two frequencies will be obvious in the frequency domain, even if they are very difficult to compute in the time domain. The FFT of each wave was computed, with significant zero padding for greater resolution and the hamming window to mitigate spectral leakage, and the peak frequency from the two peaks

was found. The beat frequency is simply defined as the difference between the two peak frequencies. The FFT analysis can be seen in fig. 10.

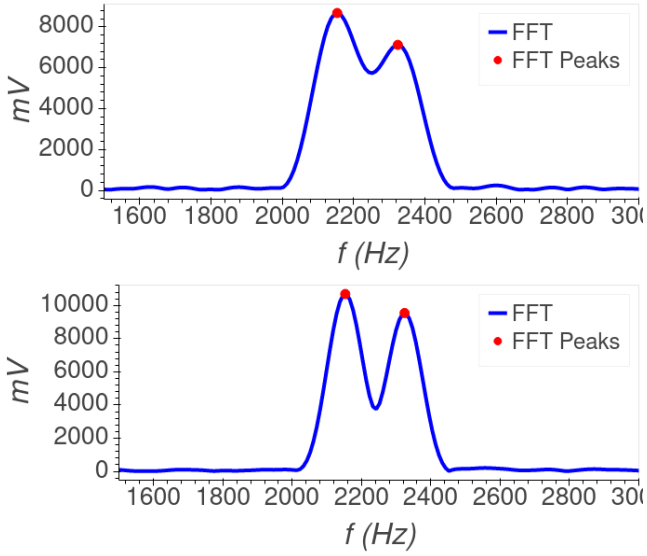

FIG. 10. Illustration of the FFT method of curve fitting the beats for both A (above) and B (below) channel waves.

The peaks for channel A were located at 2153.06 and 2323.01 Hz, corresponding to a beat frequency of 168 Hz. The peaks for channel B were located at 2153.01 and 2324.20 Hz, corresponding to a beat frequency of 171 Hz.

These beat frequency measurements for each wave were then averaged to produce a final calculated value, with the uncertainty taken as the standard deviation across each of the two measurements. These final values were 170 ± 1 Hz for channel A and 170.9 ± 0.9 for channel B.

Conclusion

A derivation in appendix D details the differential equations describing the coupled LRC circuit without damping, assuming that the electrical components used are identical. The solution to the differential equations are shown below as

$$q_+(t) = q_{+_0} sin(\omega_+ t) \tag{6}$$

$$q_-(t) = q_{-_0} sin(\omega_- t) \tag{7}$$

where $q_+ = q_1 + q_2$, $q_- = q_1 - q_2$. q_1 and q_2 are the charges on the non-coupling capacitors in the coupled LRC circuits, and ω_- and ω_+ are the frequencies of the oscillations of these capacitor charges. From the derivation in Appendix D, the frequencies ω_- and ω_+ are given by

$$\omega_+ = \frac{1}{2\pi\sqrt{LC}} \tag{8}$$

$$\omega_- = \frac{1}{2\pi\sqrt{L(C + C_{coup}}} \tag{9}$$

where L is the inductance of the two inductors, C is the capacitance of the two identical capacitors and C_{coup} is the coupling capacitance.

This system has two normal modes, as described earlier. When $q_1 = q_2$ at t = 0, $q_{-0} = 0$ the two LRC circuits operate in phase with each other. When $q_1 = -q_2$ at t = 0, $q_{+0} = 0$ the LRC circuits oscillate completely out of phase.

In the case of this experiment, $q_1 = q_0$ and $q_2 = 0$ at t = 0, because A-capacitor has been fully charged by the square wave impulse, and B-capacitor has been completely bypassed. For a coupled LRC circuit with these initial conditions the system behaves as a combination of the two normal modes.

$$q = q_0(sin(\omega_+ t) + sin(\omega_- t)) \tag{10}$$

For weak coupling, ($C_{coup} < C$), $\omega_+ \approx \omega_-$, and the normal modes are close in frequency. This gives rise to an apparent "beat" in the charges on the two capacitors. By rewriting 10 using a trigonometric identity, this beat phenomena can more clearly be understood.

$$q = 2q_0 sin[(\frac{\omega_+ + \omega_-}{2})t]cos[(\frac{\omega_+ - \omega_-}{2})t] \tag{11}$$

Equation 11 is a characteristic equation describing beats, or packets of waves. From Equation 11 the wave amplitude is determined by the sine term whereas the beat behavior is determined by the cosine term. Thus for the initial conditions $q_1 = q_0$ and $q_2 = 0$ at t = 0, with weak coupling, beats will be observed with a frequency of $\omega_+ - \omega_-$. These frequencies can be substituted to produce the beat frequency as a function of L, C, and C_{coup}.

$$f_{beat} = \frac{1}{2\pi\sqrt{LC}} - \frac{1}{2\pi\sqrt{L(C + 2C_{coup})}} \tag{12}$$

This equation can be rewritten to solve for the coupling capacitance.

$$C_{coup} = \frac{1}{2}[\frac{1}{L(\frac{1}{\sqrt{LC}} - 2\pi f_{beat})^2} - C] \tag{13}$$

Since the indicators and capacitors are identical within uncertainty, average values of L = 0.1 ± 0.003 H and C = 4.7 ± 0.1 nF were used. From these values, along with a beat frequency f_{beat} = 170 ±1 Hz, the coupling capacitance C_{coup} was calculated from Equation 14 to be 3.9 ±0.1 nF.

This calculated value agrees with the assertion that the system had weak coupling, $C_{coup} < C$,and is very similar to the measured value of 4.1 ±0.1 nF.

On a final note, the decision to analyze the falling edge of the pulse generator should be commented on. The difference in behavior between the rising edge and falling edge can be simply described as the falling edge has more oscillations. The reason for this is found in the equation for a single LRC circuit, shown below.

$$L\frac{d^2q}{dt^2} + R\frac{dq}{dt} + \frac{1}{C}q = 0 \tag{14}$$

With a non-zero voltage, the current will be much greater, meaning the resistance will dissipate proportionally more energy, resulting in more damping and fewer oscillations.

SUMMARY

In this lab, the behavior of single, uncoupled, and coupled LRC circuits were evaluated with simple relationships between L, R, C, and voltage as well as complex differential equations. The latter were simplified based on the unique initial conditions of this experiment. This behavior was further linked to a mechanical analogue, a harmonic spring system.

In the first phase of the lab, basic quantities describing the circuit and electrical components were measured directly, and calculated using curve fits which relate to solutions to the differential equations describing LRC oscillations. These values are summarized below, in Table I. In these calculations, it was observed that the precision of the DMM was responsible for virtually all of the uncertainty in our measurements.

In the second phase of the lab, the two circuits were coupled via a capacitor, which adds immense complexity to the differential equations describing the flow of charge. It was, however, possible to relate the beat frequency, or the difference in the fundamental frequency of the two circuits A and B, to the capacitance of the coupling capacitor C_coup using some assumptions related to the initial conditions of the circuits and building on more accessible solutions to these governing equations known as 'normal' operating modes.

It was possible to find this beat frequency by doing analysis on the signals from each channel in the time and frequency domain. By dividing the effect of damping out of the signals, then fitting the amplitude of the peaks, the changing amplitude of each wave was matched with a beat frequency. Separately, by simply finding the fundamental frequency of the two added waves which produce the beat using the FFT, the beat frequency could be found more directly. Both methods were considered to produce the final measure of beat frequency, 170 ± 1 Hz for each channel A and B. This agreement makes sense considering the beat is caused by the difference in each circuits own operating frequency and the other's.

Using these measurements of beat frequency, the final value for C_{coup} was calculated at 4.1 ± 0.1 nF, which is in close agreement with the measured value of 3.9 ± 0.1 nF. Given the amount of calculations needed, this value is satisfyingly close at 1 sigma. Some of this error may be due to discrepancies in the A and B circuits. If they are not perfectly identical, then the assumptions behind our equations are not accurate and the effective capacitance and resistance of the circuit, for example, will be different than expected.

TABLE I. Measured and calculated values from analysis of the two inductors in the individual LRC circuit.

Inductor Label	'A'	'B'
Full Decay Natural Frequency, ω_0	14587.05 ± 0.03 rad/s	14578.44 ± 0.03 rad/s
Damping Constant, γ	649.9 ± 0.1 s^{-1}	651.3 ± 0.1 s^{-1}
Single Period Inductance, L	0.099 ± 0.009 H	0.101 ± 0.009 H
Full Decay Inductance, L	0.100 ± 0.003 H	0.100 ± 0.003 H
Calculated Resistance, R	65 ± 2 Ω	65 ± 2 Ω
Measured Resistance, R	17.4 ± 0.5 Ω	17.2 ± 0.5 Ω
Time Constant, τ	3077.3 ± 0.6 μs	3070.9 ± 0.6 μs
Quality Factor, Q	22.4 ± 0.3	22.4 ± 0.3

TABLE II. Measured calculated values from the analysis of the coupled LRC circuits.

Property	Calculated Value	Measured Value	Deviation
LRC Capacitence	Standard / 'A': 47.1 ± 1 nF	Variable / 'B': 47.1 ± 1 nF	0σ
Beat Frequency	Circuit 'A' Beats: 170 ± 1 Hz	Circuit 'B' Beats: 170.9 ± .9 Hz	-
Coupling Capacitance	4.1 ±0.1 nF	3.9 ±0.1 nF	1σ

* smith.tr@northeastern.edu; https://github.com/trevorm4x/

[1] S. Strogatz, *"Infinite Powers: How Calculus Reveals the Secrets of the Universe"*, (Houghton Mifflin Harcourt, New York, 2019).

[2] Oregon Graduate Institute, Diffusion Theory: Fick's Laws: https://omlc.org/classroom/ece532/class5/ficks1.html

[3] Stanford, Heat Equation: https://web.stanford.edu/class/math220b/handouts/heateqn.pdf

[4] NASA, Navier-Stokes Equations: https://www.grc.nasa.gov/www/k-12/airplane/nseqs.html

[5] Wikipedia, Lenz's Law: https://en.wikipedia.org/wiki/Lenz27s$_law$